ISSN 0021-3640, JETP Letters, 2019, Vol. 109, No. 5, pp. 309–315. © Pleiades Publishing, Inc., 2019.
Published in Russian in Pis'ma v Zhurnal Eksperimental'noi i Teoreticheskoi Fiziki, 2019, Vol. 109, No. 5, pp. 312–319.

PLASMA, HYDRO- AND GAS DYNAMICS

On the Dissipation Rate of Ocean Waves due to White Capping[1]

A. O. Korotkevich[a, b, *], A. O. Prokofiev[b], and V. E. Zakharov[b, c]

[a] *Department of Mathematics and Statistics, MSC01 1115, 1 University of New Mexico, Albuquerque, NM 87131-0001, USA*
[b] *Landau Institute for Theoretical Physics, Russian Academy of Sciences, Moscow, 119334 Russia*
[c] *Department of Mathematics, The University of Arizona, P.O. Box 210089, Tucson, AZ 85721-0089, USA*
**e-mail: alexkor@math.unm.edu*

Received December 13, 2018; revised December 13, 2018; accepted December 27, 2018

We calculate the rate of ocean wave energy dissipation due to white capping by numerical simulation of deterministic phase resolving model for dynamics of ocean surface. Two independent numerical experiments are performed. First, we solve the 3D Hamiltonian equation that includes three- and four-wave interactions. This model is valid only for moderate values of the surface steepness, $\mu < 0.09$. Then we solve the exact Euler equation for non-stationary potential flow of an ideal fluid with a free surface in 2D geometry. We use the conformal mapping of domain filled with fluid onto the lower half-plane. This model is applicable for arbitrary high levels of the steepness. The results of both experiments are close. The white capping is the threshold process that takes place if the average steepness $\mu > \mu_{cr} \simeq 0.055$. The rate of energy dissipation grows dramatically with increasing steepness. Comparison of our results with dissipation functions used in the operational models of wave forecasting shows that these models overestimate the rate of wave dissipation by order of magnitude for typical values of the steepness.

DOI: 10.1134/S0021364019050035

1. INTRODUCTION

Formation of the white caps on the sea-wave crests is a well-known physical phenomenon. Its study is important for at least two reasons. White capping is a powerful mechanism of wave energy dissipation, responsible for transfer of energy and momentum from wind to water. Determination of the "dissipation function," i.e., the rate of energy and momentum transport from atmosphere to water due to white capping in the wind-driven sea, is the necessary condition for designing of an efficient operational model for wave prediction. During the last two decades, the progress in improving of accuracy of acting operational models (WAM3, WAM4, WAVEWATCH) was slow. In our opinion, the main reason for this staggering is the use of not well justified, if not just simply wrong, forms of the dissipation function. Thus, proper parametrization of the dissipation function is the question of great practical importance. At least three essentially different dissipation functions are currently used [1]. All of them are purely heuristic; none of them is justified by direct experimental or theoretical foundations.

Study of white capping is also a question of serious theoretical significance. White capping is a conspicuous example of the localized in space and time strongly nonlinear processes of wave interaction. Another key class of such phenomena is the wave collapses like self-focusing in nonlinear optics [2] or Langmuir collapse in plasma [3]. Wave collapses, like white capping, are also a mechanism for formation of hot spots of energy dissipation, but further discussion of this subject is beyond the framework of the presented article. We just mention that the theory of wave collapses is much better developed than the theory of white capping [2, 3].

From the mathematical point of view, a collapse is formation of singularity of the basic equations in a finite time. As a rule, they are described by a self-similar solution of the basic equation [2]. This solution is at least a local attractor, thus collapses have a standard universal form. The white capping is a more complicated and less studied phenomenon. A typical scenario of white capping is formation of a narrow spray ("tongue") on the crest of the breaking wave. This spray rapidly becomes unstable, turbulent and decomposes to a cloud of drops. It is not clear how universal is a form of a breaking wave. A theoretical study of white capping is enormously difficult problem (e.g., see review [4], recent paper [5] proposed detailed 2D simulation of the initial stage of foam formation).

Any possible scenario of white capping starts from dramatic growth of the surface curvature in some small localized area (for one of the mechanisms of foam formation, see recent work [5]). One can move in the reference frame where this area is resting and make a

[1] Supplementary materials are available for this article at https://doi.org/10.1134/S0021364019050035 and are accessible for authorized users.

simple and plausible conjecture: all energy and momentum captured in the white capping region will be rapidly dissipated. After accepting this conjecture, we are not interested any more in a detailed picture of the wave-breaking event. We just shall start to study this problem in terms of Fourier transform of the surface shape. In other words, the following analogy can be useful: if we throw a stone from the cliff, we know for sure that it will fall and details of stone rotation during the way to the ground are not interesting for us.

Formation of zones of high curvature means generation of "fat tails" in the spatial spectra of surface elevation. The conjecture formulated above means that all energy and momentum supplied to these tails vigorously dissipate. This phenomenon cannot be studied in a framework of the Hasselmann kinetic equation. To catch it we need to exploit any kind of dynamic (i.e., phase resolving) equations, either exact or approximate. The dissipation can be introduced in the model by addition of the artificial hyperviscosity to these equations. Such hyperviscous terms are acting only in the area of high enough wave vectors and absorbing all energy supplied to this area. In virtue of energy conservation in process of wave–wave interaction, the energy absorption in the white capping region is exactly loss for the energy containing part of spectrum. This quantity can be measured in a numerical simulation.

We realized this strategy in two independent and completely different massive numerical experiments described below. We obtained very similar, almost coinciding results leading to a fundamental conclusion that white capping is a threshold phenomenon. This is not a new idea. It was formulated by M. Banner et al. [6–8] almost two decades ago. In this paper, we present a new argument in support of this idea, obtained by straightforward numerical experiment.

In a wind driven sea, the crucial role is played by a dimensionless parameter called the steepness. There are different definitions of the steepness. If $\eta(\mathbf{r},t)$ is the shape of the surface (deviation from the unperturbed state), its dispersion σ is defined as $\sigma^2 = \langle\eta^2\rangle$. This quantity in oceanography sometimes called "energy." The natural "physical" definition of the steepness μ is

$$\mu^2 = \langle|\nabla\eta|^2\rangle, \tag{1}$$

where ∇ is the gradient computed in the plane of the fluid surface, usually *XY*-plane. This definition corresponds to an average slope of the surface. However, the "physical" steepness is hard to measure directly in a field experiment. For this reason, it is convenient to introduce the "oceanographic" steepness

$$S^2 = k_p^2\sigma^2, \tag{2}$$

where k_p is the wavenumber of the spectral peak. For pure monochromatic waves, these two definitions coincide. For real energy spectra, which in ocean have power-law "tails," they will differ: the "physical" steepness will be higher. In our experiments, spectra are relatively close to monochromatic ones, so we will not distinguish between these two definitions and use notation μ everywhere.

In accordance with already formulated concepts of M. Banner et al. [6–8], we have found that white capping (wave breaking) is the critical phenomenon with the critical steepness $\mu_{cr} \simeq 0.056$. If $\mu < \mu_{cr}$, white capping is practically absent. If $\mu \geq \mu_{cr}$, dissipation function S_{diss} is a fast growing function on $\mu - \mu_{cr}$.

This dependence of the dissipation function on the average steepness μ differs dramatically from widely accepted parametrization $S_{diss} \simeq \mu^4$ [9]. We stress once more, that our results perfectly corroborate with experimental observations made in ocean and on Lake Washington by Banner, Babanin, and Young [6–8]. They did not measure energy dissipation due to white capping but they studied probability of wave breaking event as a function of the average steepness. They obtained the same result: white capping is the critical phenomenon and the value of μ_{cr} was practically the same. The probability of wave breaking is almost zero if $\mu < \mu_{cr}$ and grows dramatically with increasing $\mu - \mu_{cr}$. This is exactly what we observed in our numerical experiments.

Our numerical results lead to a very important practical conclusion: existing operational wave forecasting models essentially overestimate the role of the white capping dissipation, especially for "mature" or relatively "old" sea, which is characterized by low μ. The dissipation function must be seriously diminished. We realize that it means total reexamination of the balance equation in the equilibrium area of spectra and choosing a more realistic model of the wind input term S_{in}. However, these questions are beyond the scope of this article.

Preliminary results of this work were published in [10]. Recently another numerical experiment using significantly simplified version of dynamical equations was published in [11]. Its results although based on different model, completely confirmed the results of this work, as well as our main conclusion: dissipation functions used in operational models overestimate contribution of white capping to waves energy absorption and must be reexamined.

2. BASIC MODELS

We study the potential flow of an ideal inviscid incompressible fluid with the velocity potential $\phi = \phi(x, y, z; t)$, satisfying the Laplace equation

$$\Delta\phi = 0. \tag{3}$$

The fluid is deep, thus we solve Eq. (3) inside the domain $-\infty < z < \eta(\mathbf{r},t)$, where $\mathbf{r} = (x, y)$ is the posi-

tion vector on the still fluid. Let $\psi = \phi|_{z=\eta}$ be the velocity potential evaluated on the surface. Fixation of $\eta = \eta(\mathbf{r},t)$, $\psi = \psi(\mathbf{r},t)$ together with condition $\phi_z \to 0$, $z \to -\infty$ define the Dirichlet–Neumann uniquely resolvable boundary condition for the Laplace equation. As shown in [12], η and ψ obey the Hamiltonian equations:

$$\frac{\partial \eta}{\partial t} = \frac{\delta H}{\delta \psi}, \quad \frac{\partial \psi}{\partial t} = -\frac{\delta H}{\delta \eta}, \tag{4}$$

where the Hamiltonian of the system has the form

$$H = \frac{1}{2}\int_{-\infty}^{+\infty} \mathrm{d}x\mathrm{d}y\left(g\eta^2 + \int_{-\infty}^{\eta} |\nabla\phi|^2 \mathrm{d}z \right).$$

Unfortunately, H cannot be written in the close form as a functional of η and ψ. However, one can limit Hamiltonian by first three terms of expansion in powers of η and ψ [12]

$$\begin{aligned} H &= H_0 + H_1 + H_2 + \ldots, \\ H_0 &= \frac{1}{2}\int (g\eta^2 + \psi\hat{k}\psi)\mathrm{d}x\mathrm{d}y, \\ H_1 &= \frac{1}{2}\int \eta\left[|\nabla\psi|^2 - (\hat{k}\psi)^2\right]\mathrm{d}x\mathrm{d}y, \\ H_2 &= \frac{1}{2}\int \eta(\hat{k}\psi)\left[\hat{k}(\eta(\hat{k}\psi)) + \eta\Delta\psi\right]\mathrm{d}x\mathrm{d}y. \end{aligned} \tag{5}$$

Here, $\hat{k} = \sqrt{-\Delta}$ is the linear integral operator in the k-space corresponding to the multiplication of Fourier harmonics ($\psi_{\mathbf{k}} = \frac{1}{2\pi}\int \psi_{\mathbf{r}} e^{i\mathbf{kr}}\mathrm{d}x\mathrm{d}y$) by $k = \sqrt{k_x^2 + k_y^2}$. For gravity waves, this reduced Hamiltonian describes four-wave interaction.

Then dynamical equations (4) acquire the form

$$\begin{aligned} \dot{\eta} &= \hat{k}\psi - (\nabla(\eta\nabla\psi)) - \hat{k}[\eta\hat{k}\psi] \\ &+ \hat{k}(\eta\hat{k}[\eta\hat{k}\psi]) + \frac{1}{2}\Delta[\eta^2\hat{k}\psi] + \frac{1}{2}\hat{k}[\eta^2\Delta\psi] - \hat{F}^{-1}[\gamma_k\eta_k], \\ \dot{\psi} &= -g\eta - \frac{1}{2}\left[(\nabla\psi)^2 - (\hat{k}\psi)^2\right] \\ &- [\hat{k}\psi]\hat{k}[\eta\hat{k}\psi] - [\eta\hat{k}\psi]\Delta\psi - \hat{F}^{-1}[\gamma_k\psi_k]. \end{aligned} \tag{6}$$

Here, dot means time derivative, $\Delta = \nabla^2$ is the Laplace operator, $\hat{F}^{-1}$ is an inverse Fourier transform, γ_k is the dissipation rate (according to [13] it has to be included in both equations), which corresponds to viscosity at small scales. The detailed description of the used numerical algorithm for solving system (6) was published in our recent work [14].

Expansion (5) is valid for full 3D problem. In the simpler 2D case dependence on y drops out and one can introduce complex coordinate $Z = x + \mathrm{i}z$, on the physical plane and perform conformal mapping onto the lower half plane $W = u + \mathrm{i}v$. The conformal mapping is completely defined by the Jacobian $R = W_Z = \frac{1}{Z_W}$. The fluid flow is defined by the complex velocity potential $\Phi = \Psi + \mathrm{i}\widehat{H}\Psi$. Here, $\widehat{H}$ is the Hilbert transform: $\widehat{H}\Psi = \frac{1}{\pi} v.p.\int_{-\infty}^{+\infty} \frac{\Psi(s)}{s-u}\mathrm{d}s$. The complex velocity is given by the equation $V = \mathrm{i}\frac{\partial\Phi}{\partial z}$. Both R and Φ are analytic functions in the lower half-plane $v < 0$. Dyachenko has shown that R and V obey the following "Dyachenko equations" [15]:

$$\begin{aligned} \frac{\partial R}{\partial t} &= \mathrm{i}(UR' - RU'), \\ \frac{\partial V}{\partial t} &= \mathrm{i}(UV' - RB') + g(R-1). \end{aligned} \tag{7}$$

Here, $U = P^-(R\bar{V} + \bar{R}V)$ and $B = P^-(V\bar{V})$, where $P^- = 1/2(1 + \mathrm{i}\widehat{H})$ is the operator of projection to the lower half-plane. We must stress that Eqs. (7) are **exact** equations, completely equivalent to the primordial Euler equations. In this work, we used numerical algorithm analogous to the one used in [16].

3. EXPERIMENTAL RESULTS

3.1. 3D Experiment

We simulate primordial dynamical Eqs. (6) in a $2\pi \times 2\pi$ periodic box with spectral resolution 512×4096. We did not impose any external forcing but studied decay of initially created wave turbulence, which is almost unidirectional swell and can be simulated in such rectangular spectral domain due to strong anisotropy of the wave field. We used the following damping parameters:

$$\gamma_k = \begin{cases} 0, k < k_d, \quad k_d = 1024, \\ -\gamma(k-k_d)^2, k \geq k_d, \ \gamma = 2.86\times10^{-3}. \end{cases} \tag{8}$$

Gravitational acceleration was $g = 1$ and the time step was $\Delta t = 4.23\times10^{-4}$.

As initial conditions, we used Gauss-shaped spectrum, centered at $\mathbf{k}_0 = (0;100)$ with the width $D_i = 30$. All harmonics amplitudes were random Gaussian values with the following average

$$\begin{cases} |a_{\mathbf{k}}| = A_i \exp\left(-\frac{1}{2}\frac{|\mathbf{k}-\mathbf{k}_0|^2}{D_i^2}\right), & |\mathbf{k}-\mathbf{k}_0| \leq 2D_i, \\ |a_{\mathbf{k}}| = 10^{-12}, & |\mathbf{k}-\mathbf{k}_0| > 2D_i. \end{cases} \tag{9}$$

Here, $a_{\mathbf{k}} = \sqrt{\frac{\omega_k}{2k}}\eta_{\mathbf{k}} + \mathrm{i}\sqrt{\frac{k}{2\omega_k}}\psi_{\mathbf{k}}$ are normal variables [14]. Phases were random numbers uniformly distributed in the interval $[0;2\pi)$. The value of A_i was varying in order to provide the desired initial average steepness

$\mu = \sqrt{\langle|\nabla\eta(\mathbf{r})|^2\rangle}$, which was in the interval from 0.05 to 0.09.

During the experiment, we observed dynamics of initial spectral distribution during time $100T_0$, where T_0 is the period of the wave corresponding to spectral maximum. This time is approximately 10 nonlinear times and we suppose that at this time initial spectral distribution is relaxed close enough to a quasistationary self-similar state. This means formation of power-law Kolmogorov–Zakharov (KZ) spectral tails [17, 18], which are routinely observed in field and laboratory experiments, e.g., see [19].

We have approximately one decade inertial interval in wavenumbers. It lets us to observe formation of a long spectral tail and to secure our spectral maximum from the direct influence of the dissipation region. We would like to stress, that this is not far from reality. In the wind-driven sea, the inertial interval for gravity waves is posed approximately in the range (see [19])

$$\omega_p < \omega < 3.5\omega_p,$$

where ω_p is the spectrum peak circular frequency corresponding to the wavenumber k_p. This spectral band is broad enough to provide a possibility for formation of sharp crests, where the local steepness is much higher than average, which could lead to breakdown of our dynamical Eqs. (6), derived in assumption that we can expand Hamiltonian in powers of the steepness, so it gives a limitation on the value of the initial average steepness. We also have to keep the average steepness high enough to secure four wave interaction from been stopped by discreteness of the wavenumbers grid [20]. To achieve a balance between these two requirements was the main problem during the experiment.

In the process of the experiment, we calculated the inverse normed time of wave action derivative:

$$\gamma_{\text{diss}} = \frac{N'}{\omega_0 N} = 2\frac{N(t+10T_0) - N(t)}{10T_0\omega_0(N(t+10T_0) + N(t))},$$

where $\omega_0 = \sqrt{gk_0}$, which was calculated at three different times $t = 70T_0$, $80T_0$, and $90T_0$. Because initial wave field was stochastic in the first approximation, we can consider these three results as three experiments with random initial phase and amplitude, or three independent cases in stochastic ensemble. The results of this experiment are presented in Fig. 1.

Let us mention that at $\omega \simeq 3.5\omega_p$ the KZ spectrum tails $\sim\omega^{-4}$ transit at least at some conditions to the Phillips spectrum $\sim\omega^{-5}$ [21, 22]. This transition needs to be studied more carefully. Some preliminary results can be found in [23, 24].

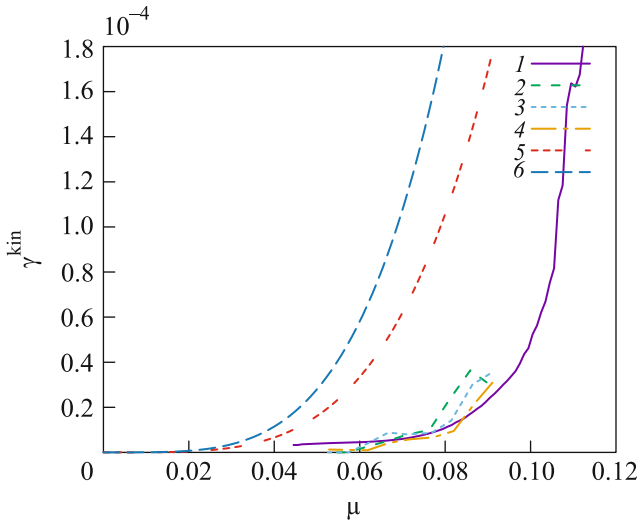

Fig. 1. (Color online) Dissipation term γ_{diss} versus the average surface steepness according to (*1*) 2D fully nonlinear experiment; (*2*) 3D experiment, where the derivative was computed on a period of time from $70T_0$ to $80T_0$; (*3*) 3D experiment, where the derivative was computed on a period of time from $80T_0$ to $90T_0$; (*4*) 3D experiment, where the derivative was computed on a period of time from $90T_0$ to $100T_0$; (*5*) $2.58\mu^4$, which corresponds to the WAM3 model for the $\delta(\mathbf{k})$ wave packet; and (*6*) $4.48\mu^4$, which corresponds to the WAM4 model for the $\delta(\mathbf{k})$ wave packet.

3.2. 2D Experiment

In this experiment, we solved Dyachenko equations (7) in the periodic spatial domain of length 2π with spectral resolution of 8192 harmonics. We replaced in equations for R and V time derivative by:

$$\frac{\partial}{\partial t} := \frac{\partial}{\partial t} - \gamma_p(k) + 2.0\times10^{-12}k^4. \qquad (10)$$

Here, $\gamma_p(k)$ is the pumping function symmetric in the k-space concentrated near $k = k_0 = 35$. As initial data, we chose $R = 1$, V is white noise consisting of harmonics with random phase and amplitude 10^{-20}.

On the initial stage of experiment, pumping forms quasimonochromatic standing wave of a very high steepness $\mu = \sqrt{\langle(\eta'(x))^2\rangle} \simeq 0.2$. Then, we switched off the pumping and measured $\gamma_{\text{diss}} = \dfrac{N'}{\omega_p N}$, where ω_p is the frequency at k_p. The idea was to reach steepnesses beyond the range of applicability of truncated 3D model and observe the dissipation there, eventually bringing the solution to the values of steepness manageable by 3D experiment. We observed fast dissipation that slowed down dramatically when the steepness achieved $\mu \simeq 0.1$. The dissipation rate for small steep-

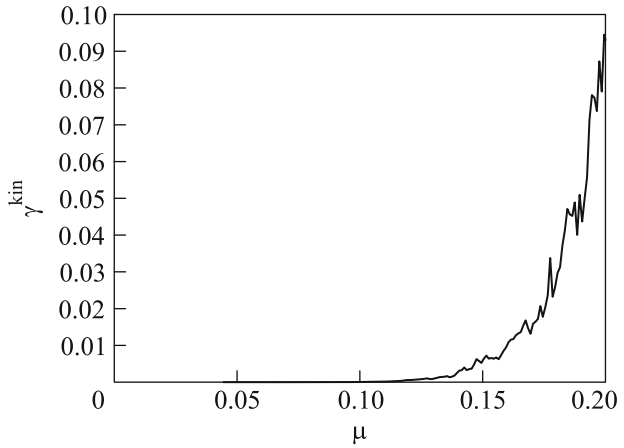

Fig. 2. Dissipation term γ_{diss} versus the average surface steepness $\mu = \sqrt{\langle|\eta'(x)|^2\rangle}$.

nesses is presented in Fig. 1 together with the results of the 3D experiment.

The dissipation rate for higher steepnesses is given in Fig. 2. One can see that steep waves loose energy extremely fast, during few wave periods.

3.3. Comparison with Wave Forecasting Models

Widely used wave forecasting models WAM3 and WAM4 utilize the following dissipation functions depending on the wavenumber k:

$$\gamma_{\mathbf{k}} = C_{ds}\tilde{\omega}\frac{k}{\tilde{k}}\left((1-\delta)+\delta\frac{k}{\tilde{k}}\right)\left(\frac{S}{S_{PM}}\right)^{p}, \qquad (11)$$

where k and ω are the wavenumber and frequency, respectively; tilde denotes mean value; C_{ds}, δ, and p are tunable coefficients; $S = k_p\sigma$ is the "oceanographic" steepness; and $S_{PM} = (3.02 \times 10^{-3})^{1/2}$ is the value of $\tilde{S}$ for the Pierson–Moscowitz spectrum. The tunable coefficients for the WAM3 case are:

$$C_{ds} = 2.35\times10^{-5}, \quad \delta = 0, \quad p = 4 \qquad (12)$$

and for the WAM4 case are:

$$C_{ds} = 4.09\times10^{-5}, \quad \delta = 0.5, \quad p = 4. \qquad (13)$$

As long as we are interested only in rough estimate, we can identify $S \simeq \mu$ and consider the spectrum as completely concentrated near the spectral maximum $k = \tilde{k}$, $\omega = \tilde{\omega}$. As a result, we end up with following normalized dissipation rates $\gamma_{\text{diss}} \simeq 2.58\mu^4$ for WAM3 and $\gamma_{\text{diss}} \simeq 4.48\mu^4$ for WAM4. Corresponding curves are plotted in Fig. 1. One can see that for typical wind driven sea steepness $\mu \simeq 0.06$ they overestimate the dissipation due to white capping by almost order of magnitude.

We must stress that we observed the "threshold type" onset of dissipation only in the case when spectral peak scale k_p and beginning of dissipation scale k_d are separated far enough in k-space. If they are relatively close to each other (say, $k_d \sim 3k_p$ or $k_d \sim 5k_p$, we performed both these experiments) we observe a smooth power-law dependence of dissipation on the steepness, similar to what was offered in WAM3 model. This is due to drain of energy from the spectral peak through slave harmonics in dissipation range. Such a dependence can be obtained analytically ($p = 4$ for the case $k_d \sim 3k_p$). It has to be noted that these scales in the real wind-driven sea are separated by at least an order of magnitude.

4. DISCUSSION AND RESULTS

One could ask a question: "Why did the authors use these two models with such different initial conditions?" The answer is simple. If the mechanism of dissipation which we proposed (domination of generation of multiple harmonics, when local singularities start to appear, aided by direct cascade energy transfer) is universal, then results in these two models (just a reminder, four-wave resonant interactions are absent in 2D case, which means different nonlinear interaction physics; while multiple harmonics generation is the same) will be not necessarily the same but close. In addition, using fully nonlinear 2D model we can reach range of steepnesses corresponding to rough sea. As we expected, simulations suggest that the mechanism is universal. Results are discussed in details below.

First, both our experiments clearly show that dissipation functions widely used in operational wave forecasting models dramatically overestimate the role of white capping in the energy balance of wind-driven sea. Other, less direct reasons, in virtue of this statement were formulated in [4].

Comparison of 3D and 2D experiments for "realistic" steepnesses $0.06 < \mu < 0.08$ shows that in 3D case the dissipation is somewhat stronger. This fact has a natural explanation. As mentioned above, there are two completely different mechanisms of energy transfer to the small-scale region of the spectrum where waves dissipate. One is the Kolmogorov-type flux of energy due to four-wave resonant processes (see, e.g., [25]). Second is the direct formation of white caps on crests of waves. Strong local nonlinearity leads to fast growth of multiple harmonics, which is much faster than energy cascade. In 2D geometry only second mechanism is working. We cannot compare efficiency of these two mechanisms for high steepnesses ($\mu > 0.08$) because for such steep waves any type of weakly nonlinear models fail. Meanwhile, 2D experiments show that the white capping dissipation of steep waves (since $\mu \simeq 0.1$) is an extremely powerful process, and the waves close to the critical Stokes wave ($\mu > 0.3$) just cannot exist in reality. They break up

very rapidly. The mechanism of regularization of such process through formation of limiting capillary waves on the crest was recently modeled and described in [5].

Our 3D experiments confirmed the idea of Banner et al. [7] about "threshold" character of white capping. There are several experimental evidences in support of comparison of the wave-breaking phenomenon with second-order phase transition (e.g., see [23]). The threshold level $\mu_{cr} \simeq 0.055$ coincides with experimental data [4, 7] very well. The results of the 2D experiment are less evident. As seen in Fig. 1, some dissipation remains even for waves of a small steepness. This remainder of dissipation does not depend on the steepness at all. This is a numerical artifact. We were not able to stabilize our numerical scheme without introducing of artificial hyperviscosity in the whole k-space. Recent experiments [11] performed in a framework of a less accurate (and more robust) model of 2D waves support the threshold nature of white capping.

Our next task is formulation of a dissipation function, more realistic than (11). The first step in this direction was made in [24]. Here, we propose as a first preliminary results nonlinear least square (Marquardt–Levenberg algorithm implementation in Gnuplot [26]) fits of two functions. Probably the most interesting is the region of relatively small steepnesses corresponding to mature or not so rough sea ($0.055 \le \mu \le 0.1$). We tried two types of functions, exponential:

$$\gamma_k^{\text{lowExp}}(\mu) = (1.248 \times 10^{-7}) \exp(59.40\mu), \qquad (14)$$

and polynomial in terms of the difference $\mu - \mu_{cr}$:

$$\gamma_k^{\text{lowPoly}}(\mu) = (1.040 \times 10^{-2})|\mu - 0.055|^{1.756}. \qquad (15)$$

For steepnesses corresponding to rough sea (up to $\mu = 0.2$), we obtained different fits. Exponential function yielded the dependence

$$\gamma_k^{\text{highExp}}(\mu) = (8.679 \times 10^{-7}) \exp(58.00\mu), \qquad (16)$$

and polynomial fit gave this result:

$$\gamma_k^{\text{highPoly}}(\mu) = (1.468 \times 10^{5})|\mu - 0.055|^{7.398}. \qquad (17)$$

It should be stressed, that this choice of functions is kind of random. The measured dependences of dissipation on the steepness for every experiment are given in the supplementary materials for this article, so anybody can try to choose any function and fit it using any readily available package.

Having said that, let us describe the format and the files in the supplementary materials. All of them are plain text files, which contain two columns: the first is the average steepness and the second is the measured dissipation rate γ. The file mu_gamma_3D.data in the supplementary materials contains data points from 3D experiments. For every experiment we averaged three values obtained from time intervals $80–70T_0$, $90–80T_0$, and $100–90T_0$ as it is described in corresponding section above. Both values of the steepness and dissipation rate were averaged. File mu_gamma_2D.data in the supplementary materials contains data points from 2D experiments. One can see that artificial viscosity for steepnesses $\mu < 0.065$ affects the data as discussed in details above. This is why we decided to glue together both sets and use all data points from the 3D case together with data points for a higher steepness from the 2D case for purposes of fitting some functions to the dependence. This combined data set is given as the file mu_gamma_2D_3D.data in the supplementary materials. We hope that these initial results can be used by community in order to improve dissipation functions currently used in different wave forecasting models.

This work was supported by the Russian Academy of Sciences (program no. 0033-2018-0014). A.O. Korotkevich acknowledges the support of the U.S. National Science Foundation (grant no. OCE 1131791). Analysis of the experimental data was performed by A.O. Korotkevich and was supported by the Council of the President of the Russian Federation for State Support of Young Scientists and Leading Scientific Schools (project no. NSh-9697.2016.2).

REFERENCES

1. H. L. Tolman, *User Manual and System Documentation of WAVEWATCH III* (U. S. Dept. of Commerce, Natl. Ocean. Atmos. Administration, Natl. Weather Service, Natl. Centers for Environmental Prediction, 2009).
2. C. Sulem and P.-L. Sulem, *The Nonlinear Schrödinger Equation: Self-Focusing and Wave Collapse* (Springer, New York, 1999).
3. V. E. Zakharov, Sov. Phys. JETP **35**, 908 (1972).
4. A. Pushkarev and V. E. Zakharov, Ocean Model. **103**, 18 (2016).
5. S. A. Dyachenko and A. C. Newell, Stud. Appl. Math. **137**, 199 (2016).
6. M. L. Banner and X. Tian, J. Fluid Mech. **367**, 107(1998).
7. M. L. Banner, A. V. Babanin, and I. R. Young, J. Phys. Oceanogr. **30**, 3145 (2000).
8. J.-B. Song and M. L. Banner, J. Phys. Oceanogr. **32**, 2541 (2002).
9. G. J. Komen, L. Cavaleri, M. Donelan, K. Hasselmann, and P. A. E. M. Janssen, *Dynamics and Modelling of Ocean Waves* (Cambridge Univ. Press, Cambridge, UK, 1994).
10. V. E. Zakharov, A. O. Korotkevich, and A. O. Prokofiev, AIP Conf. Proc. **1168**, 1229 (2009).
11. A. I. Dyachenko, D. I. Kachulin, and V. E. Zakharov, JETP Lett. **102**, 513 (2015).
12. V. E. Zakharov, J. Appl. Mech. Tech. Phys. **9**, 190 (1968).
13. F. Dias, A. I. Dyachenko, and V. E. Zakharov, Phys. Lett. A **372**, 1297 (2008).
14. A. O. Korotkevich, A. I. Dyachenko, and V. E. Zakharov, Phys. D (Amsterdam, Neth.) **321–322,** 51 (2016).

15. A. I. Dyachenko, Dokl. Math. **63**, 115 (2001).
16. V. E. Zakharov, A. I. Dyachenko, and A. O. Prokofiev, Eur. J. Mech. B: Fluids **25**, 677 (2006).
17. A. I. Dyachenko, A. O. Korotkevich, and V. E. Zakharov, JETP Lett. **77**, 546 (2003).
18. A. I. Dyachenko, A. O. Korotkevich, and V. E. Zakharov, Phys. Rev. Lett. **92**, 134501 (2004).
19. M. A. Donelan, J. Hamilton, and W. H. Hui, Phil. Trans. R. Soc. London, Ser. A **315**, 509 (1985).
20. V. E. Zakharov, A. O. Korotkevich, A. Pushkarev, and A. I. Dyachenko, JETP Lett. **82**, 487 (2005).
21. A. O. Korotkevich, Phys. Rev. Lett. **101**, 074504 (2008).
22. A. O. Korotkevich, Math. Comput. Simul. **82**, 1228 (2012).
23. A. C. Newell and V. E. Zakharov, Phys. Rev. Lett. **69**, 1149 (1992).
24. V. E. Zakharov and S. I. Badulin, arXiv:1212.0963.
25. V. E. Zakharov, Phys. Scripta T **142**, 014052 (2010).
26. Gnuplot, Command-Driven Interactive Function Plotting Program 1986–2018. http://gnuplot.info.